Stabilization of Uncertain Parabolic PDE Systems Under Weighted Try-Once-Discard Protocol With Actuator Failures

Jinliang Liu, *Senior Member, IEEE*, Lijuan Zha, Wen Jiang, and Engang Tian, *Senior Member, IEEE*

***Abstract*—This article investigates the output feedback stabilization problem for a parabolic partial differential equation (PDE) system with uncertain parameters, which is subject to limited communication resources. First, to alleviate the burden of channel communication and avert data collision, the multichannel measurement outputs are scheduled by the weighted try-once-discard protocol. Moreover, to bridge the gap between theory and reality, the Markov process is utilized to depict the occurrence of various actuator faults in a stochastic manner. An impulsive closed-loop model is established in light of the network-induced delay and various stochastically occurring actuator faults. Following the model, sufficient criteria for guaranteeing the input-to-state stability of the PDE system are put forward by constructing a new Lyapunov functional. Then, one can deduce the determination of the controller gains and weighted matrices by employing the technique of linearizing the matrix inequalities. Finally, simulation results unequivocally demonstrate the effectiveness of the proposed method.**

***Index Terms*—Markov jump actuator fault, partial differential equation (PDE), uncertain system, weighted try-once-discard (WTOD) protocol.**

I. Introduction

In RECENT years, partial differential equations (PDEs) have been extensively used to model the distributed parameter systems (DPSs) [1], [2], owing to their advantages in describing the spatiotemporal distribution characteristics in most modern industrial processes, such as heat transfer, fluid dynamics, and electromagnetic fields. The infinite-dimensional nature of PDEs presents significant challenges in the analysis and control of DPSs. Various types of PDE systems are currently emerging as research hotspots, including parabolic PDE systems [3], hyperbolic PDE systems [4], and elliptic PDE systems [5]. Moreover, in industrial applications, we frequently encounter challenges associated with uncertainty, typically resulting from errors in input data, variations in boundary conditions, inaccuracies in model parameters, and responses to external disturbances [6], [7], [13]. This complicates accurate modeling and reliable prediction of the behavior of PDE systems [9]. Therefore, it is imperative to develop effective control strategies that ensure the stability and robustness of parabolic PDE systems with uncertain parameters.

In practical control systems, actuator faults can not be overlooked, which may arise from mechanical wear, circuit malfunctions, or external interference in practical scenarios. If an actuator experiences the fault, it may fail to execute the corresponding actions accurately according to the control commands, leading to a decline in the functionality of the control system and an inability to meet the expected control requirements. Hence, it is crucial to develop effective fault-tolerant control (FTC) methods to address actuator failures. Over the past few years, there has been a noteworthy upswing in attention toward FTC [8], [10], [11], [12]. For instance, the FTC problem of delayed PDE systems under spatially point measurements is addressed in [11] to handle the actuator failures. This study considers the impact of both the loss of the original control signal and the presence of fault signals. Li et al. [12] proposed the utilization of a smoothing function-based compensation term to effectively mitigate the influence caused by the actuator failures in a cascaded partial differential equation (PDE)–ordinary differential equation (ODE) system. Despite the significant advancements in FTC for PDE systems, there is a dearth of research specifically addressing output feedback FTC for parabolic PDE systems with uncertain parameters.

In practical applications, as the complexity of controlled objects continues to increase, there is a corresponding rise in the volume of data that need to be transmitted between sensors and remote controllers. Existing control strategies are mostly based on the assumption of normal data transmission [3]. However, in reality, network congestion, conflicts, and other issues stemming from limited network bandwidth frequently arise, significantly compromising the effectiveness of these control methods.

Received 5 November 2024; revised 25 January 2025; accepted 18 March 2025. Date of publication 14 April 2025; date of current version 13 June 2025. This work was supported in part by the National Natural Science Foundation of China under Grant 62373252, and Grant 62273174 and in part by the Natural Science Foundation of Jiangsu Province of China under Grant BK20230063. Paper no. TII-24-5806. *(Corresponding author: Lijuan Zha.)*

Jinliang Liu is with the School of Computer Science, Nanjing University of Information Science and Technology, Nanjing 210044, China (e-mail: 003768@nuist.edu.cn).

Lijuan Zha is with the School of Science, Nanjing Forestry University, Nanjing 210037, China (e-mail: zhalijuan@njfu.edu.cn).

Wen Jiang is with the College of Information Engineering, Nanjing University of Finance and Economics, Nanjing 210023, China (e-mail: 1120220513@stu.nufe.edu.cn).

Engang Tian is with the School of Optical-Electrical and Computer Engineering, University of Shanghai for Science and Technology, Shanghai 200093, China (e-mail: teg@usst.edu.cn).

Digital Object Identifier 10.1109/TII.2025.3556063

To mitigate the negative impact of bandwidth constraints on controller performance, some researchers have utilized communication protocol scheduling for data transmission, including the weighed try-once-discard (WTOD) protocol, random access (RA) protocol, and round-robin (RR) protocol. The advantages of RA protocol and RR protocol lie in their simplicity and the capability to provide relatively fair resource allocation. However, they lack the capability to dynamically adjust data transmission based on real-time system status. WTOD protocol [16], [17] dynamically selects the data that need to be transmitted by measuring the magnitude of sensor data changes. Under WTOD protocol, the transmitted data of the sensor nodes are based on "competition," only one sensor nodes can have access to the network, which mitigates network congestion effectively. WTOD protocol has been adopted in many controller or filter design problem. However, the majority of the the existing achievements are based on discrete systems, which cannot be applied to the continuous systems, not to mention the parabolic PDE systems. Therefore, the utilization of WTOD protocol in continuous PDE systems remains a novel and challenging research topic.

Inspired by the above content, this article focuses on a PDE-based networked control system (NCS) with multiple channels, utilizing the output feedback control method. First, the WTOD scheduling scheme is employed to coordinate the priorities of nodes access to the network. Then, considering network-induced delays and actuator failures, a pulse-closed-loop model of the PDE-based NCS is established. Sufficient conditions are obtained to ensure the stability of the pulse system. The novelties of this article can be categorized as threefold.

1) In previous scholarly works, PDE systems typically employ control strategies, such as sampled measurement [18], quantized transmission [19], [20], and piecewise control [21] to mitigate transmission and control costs. To further optimize the control strategy, WTOD protocol is incorporated into schedule nodes.
2) The mode switching of actuator failures affected by their own faults and external disturbance signals is modeled as a Markov process, which can demonstrate the stochastic nature of actuator failures in contrast to conventional ones [22], thereby highlighting their inherent randomness.
3) Although WTOD protocol has been adopted in some publications, most of the results are developed for discrete systems. Besides, the current achievements in FTC for PDE systems with actuator failures suppose the network resources are abundant and network congestion is not taken into account, which have limitations. In this article, we first investigate the FTC control for the PDE system with WTOD protocol and actuator faults.

Notations: $\mathbb{R}^n$ and $\mathbb{R}^{n\times m}$ denote the n-dimensional Euclidean space and $n \times m$-dimensional matrix. diag$\{\dots\}$ and col$\{\dots\}$ means the block-diagonal matrix and block-column vector, respectively. Matrix $P > 0$ means that P is a positive definite symmetric matrix and symbol $*$ refers to the symmetric terms in a symmetric matrix. $\mathbf{x}^T$ is the transpose of the matrix $\mathbf{x}$ and $\mathbf{x}^{-1}$ represents the inverse of $\mathbf{x}$. $\lambda_{\min}(P_m)$ denotes the minimum eigenvalue of matrix P_m. $|\cdot|$ represents the euclidean norm of a vector. For simplicity, we define $z(x,t) \triangleq z$, $y(x,t) \triangleq y$, $e(x,t) \triangleq e(t)$, $z_t \triangleq \frac{\partial z(x,t)}{\partial t}$, $z_{xx} \triangleq \frac{\partial^2 z(x,t)}{\partial x^2}$, $y(x,\cdot) \triangleq y(\cdot)$, and $\vec{y}(x,\cdot) \triangleq \vec{y}(\cdot)$.

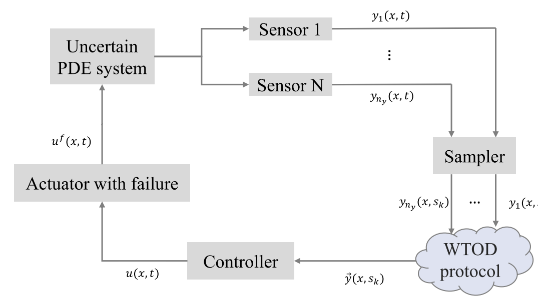

Fig. 1. Framework of uncertain PDE system under WTOD protocols.

II. Problem Formulation

A. Plant and Sampler

As illustrated in Fig. 1, consider the uncertain linear parabolic PDE system as follows:

$$\begin{cases} z_t = z_{xx} + (A + \Delta A)z + Bu^f(x,t) \\ y = Cz \end{cases} \tag{1}$$

with the Neumann boundary conditions

$$z_x(l_1,t) = 0, \quad z_x(l_2,t) = 0 \tag{2}$$

and the initial condition

$$z(x,0) = z_0(x) \tag{3}$$

where $z(x,t) \in \mathbb{R}^{n_z}$ is the state vector; $x \in [l_1, l_2]$ and t represent spatial position and time, respectively; $u^f(x,t) \in \mathbb{R}^{n_u}$ is the control input signal influenced by stochastic actuator failure, and $y(x,t) = [y_1^T(x,t),\dots,y_N^T(x,t)]^T \in \mathbb{R}^{n_y}$ is the measurement output. A, B, $C = [C_1^T,\dots,C_N^T]^T$ are constant matrices with appropriate dimensions. ΔA is an uncertain matrix satisfying $\Delta A = HF(x,t)E$, in which H, $F(x,t)$, and E are known matrices with the limitation of $F(x,t)^T F(x,t) \le I$.

Denote s_k as sampling instant, $k \in \mathbb{Z}, \mathbb{Z} = \{0,1,2,\dots\}, s_0 = 0$. It is assumed that the upper bound of the sampling interval is v, that is $s_{k+1} - s_k \le v$.

B. Time Delay and WTOD Protocol

In this article, we presume that there is a delay in transmitting the measurement output from the sampler to the controller. Considering that different channels operate in varied environments, $\eta_i^{\sigma_k} \in [\tilde{\eta}_m, \tilde{\eta}_M]$ is introduced to represent the time-varying time delay of channel i at sampling time s_k.

To alleviate network congestion and conflicts, it is stipulated that only one channel is permitted to transmit data at each sampling instant. The active node at instant s_k is denoted by σ_k, thus we have $t_k = s_k + \eta_i^{\sigma_k}$. To put it differently, at sampling instant s_k, channel σ_k can send updated output information $y_i(x, s_k)$ and other channels will be in a dormant state. As compensation, the controller will adopt the previous measurement output

$$\vec{y}(x, s_k) = \begin{cases} y_i(x, s_k), & i = \sigma_k \\ \vec{y}_i(x, s_{k-1}), & i \neq \sigma_k. \end{cases} \tag{4}$$

Define the scheduling error

$$e_i(t) = \vec{y}_i(x, s_{k-1}) - y_i(x, s_k), \quad t \in [t_k, t_{k+1}) \tag{5}$$

where $e(t) = \text{col}\{e_1, \ldots, e_N\}^T \in \mathbb{R}^{n_y}$, $\vec{y}(s_{-1}) \triangleq 0$.

Given the influence of communication network bandwidth, WTOD protocol [23] is employed to select active node for $t \in [t_k, t_{k+1})$

$$\sigma_k = \min \arg \max_{i=1,2,\ldots,N} e_i^T(t) Q_i e_i(t) \tag{6}$$

where Q_i are weighted matrices to be determined later.

Remark 1: This article introduces the WTOD protocol for scheduling signal transmission between sensors and remote controller. At each sampling instant, the WTOD protocol determines which sensor nodes should transmit their data, taking into account the assigned weights and the current network conditions. This ensures that critical or high-priority data are prioritized for transmission, while less important or redundant data may be deferred to conserve resources.

C. Controller and Actuators With Stochastic Failure

Based on the measurement output received by the controller, we design the controller as follows:

$$u(x,t) = K\vec{y}(x, s_k), \quad t \in [t_k, t_{k+1}) \tag{7}$$

where $K = [K_1, K_2, \ldots, K_N]$ represents the controller gain to be determined later.

Taking into account the practical scenario where actuators may experience malfunctions and random failures, $u(x,t)$ is updated to the following form:

$$u^f(x,t) = F(\beta(t))u(x,t) + L(\beta(t))v(x,t) \tag{8}$$

where $F(\beta(t)) \in [0,1]$, $L(\beta(t)) \in \{0,1\}$ represents the severity of fault, $v(x,t) \in \mathbb{R}^{n_u}$ is randomly generated fault signal, satisfying

$$\int_0^t \int_{l_1}^{l_2} v^T(x,t)v(x,t)\text{d}x\text{d}t \leq J^2 \tag{9}$$

and $\beta(t) \in \{1, 2, \ldots, M\}$ indicates that there are M types of failure conditions. Assume the value of $\beta(t)$ is determined by a continuous homogeneous Markov process with the following transition rate:

$$\begin{aligned} &P_r\{\beta(t+\Delta t) = n \mid \beta(t) = m\} \\ &= \begin{cases} \pi_{mn}\Delta t + o(\Delta t), & m \neq n \\ 1 + \pi_{mm}\Delta t + o(\Delta t), & m = n \end{cases} \end{aligned} \tag{10}$$

where $\Delta t > 0$, $\lim_{\Delta t \to 0}[o(\Delta t)/\Delta t] = 0, \pi_{mn} \geq 0 (m \neq n)$, and $\sum_{n=1}^{M} \pi_{mn} = 0, m \in \{1, 2, \ldots, M\}$. Denote the transition rate matrix as $\Pi \triangleq [\pi_{mn}]_{M \times M}$.

With the purpose of simplifying the derivation, $F(\beta(t) = m)$ and $L(\beta(t) = m)$ are simplified to F_m and L_m, respectively.

Remark 2: The construction of M fault modes is based on Markov processes. The failure model utilized in this article considers both the inherent failures of the actuator and the influence of external error signals on the actuator. By setting different transition matrices, various types of faults can be flexibly reflected. The stochasticity and uncertainty of Markov processes align with the random nature of the fault occurrences in practical systems.

Remark 3: The randomly occurring actuator faults are represented as a fault model based on a Markov jump process. Employing different parameters to denote the occurrence of different failure cases. For example, when $F_m = 1$ and $H_m = 0$, it indicates that the actuator is functioning normally; $F_m = 0$ and $H_m = 1$ represent a stuck fault. $0 < F_m < 1$ and $H_m = 0$ signify the partial failure of the actuator. $F_m = 0$ and $H_m = 0$ denote an interrupted fault. Finally, when $F_m = 1$ and $H_m = 1$, it indicates a biased fault.

Considering the random failures, the controller gain corresponding to the mth fault mode is designed as $K = [K_{1m}, K_{2m}, \ldots, K_{Nm}]$.

D. Impulsive Model and Problem Description

By the definition of scheduling error in (5), we have

$$\begin{aligned} &e_i(x, t_{k+1}) \\ &= \begin{cases} C_i(z(x, s_k) - z(x, s_{k+1})), & i = \sigma_k \\ e_i(x, t_k) + C_i(z(x, s_k) - z(x, s_{k+1})), & i \neq \sigma_k \end{cases} \end{aligned} \tag{11}$$

and (4) can be reformulated as

$$\vec{y}(x, s_k) = \begin{cases} C_i z(x, s_k), & i = \sigma_k \\ e_i(x, t_k) + C_i z(x, s_k), & i \neq \sigma_k. \end{cases} \tag{12}$$

Substitute (12) into (8)

$$\begin{aligned} u^f(x,t) &= F(\beta(t))K\vec{y}(x, s_k) + L(\beta(t))v(x,t) \\ &= F(\beta(t))K\left(Cz(x, s_k) + \sum_{i=1, i\neq\sigma_k}^{N} I_i e_i(x,t)\right) \\ &\quad + L(\beta(t))v(x,t) \end{aligned} \tag{13}$$

where $I_i = \text{col}\{\underbrace{0, \ldots, 0}_{i-1}, I, \underbrace{0, \ldots, 0}_{N-i}\}$.

Define $\tau(t) = t - s_k$, $t \in [t_k, t_{k+1})$. Considering $s_{k+1} - s_k \leq v$ and $\eta_i^{\sigma_k} \in [\tilde{\eta}_m, \tilde{\eta}_M]$, one can get $\tilde{\eta}_m \leq t - s_k \leq v + \tilde{\eta}_M$. Denote $v + \tilde{\eta}_M \triangleq \tau_M$, we can get an upper and lower bound on $\tau(t)$, that is, $\tilde{\eta}_m \leq \tau(t) \leq \tau_M$.

Then, the close-loop PDE system can be obtained by

$$\begin{aligned} &z_t = z_{xx} + (A + \Delta A)z + BF(\beta(t))KCz(x, t - \tau(t)) \\ &+ BF(\beta(t))K \sum_{i=1, i\neq\sigma_k}^{N} I_i e_i(x,t) + BL(\beta(t))v(x,t). \end{aligned} \tag{14}$$

Definition 1: The PDE system (14) is said to be input-to-state stability (ISS) if there exist constants $b > 0$ and $\kappa > 0$ such that for $t \geq t_0$ the following:

$$|z(x,t)|^2 \leq be^{-\kappa(t-t_0)}\left[|z(x,t_0)|^2 + |e(x,t_0)|^2\right] \tag{15}$$

$$|e(x,t)|^2 \leq be^{-\kappa(t-t_0)}\left[|z(x,t_0)|^2 + |e(x,t_0)|^2\right] \tag{16}$$

holds for the solutions of the PDE system initialized with $z_{t_0} = z(x,t_0)$ and $e(x,t_0)$.

This article aims to deduce sufficient conditions for the ISS of the uncertain PDE system under time delay, WTOD protocol, and actuator failure. Then, the controller gain is calculated in accordance with the sufficiency condition.

To develop the main results, several necessary lemmas are listed.

Lemma 1 ([24]): For any constant symmetric matrix $Q \in \mathbb{R}^{m\times m}$, scalar $\lambda > 0$, vector function $\omega : [0,\lambda] \to \mathbb{R}^m$ such that the integration concerned are well defined, then

$$\lambda \int_0^{\lambda} \omega(\alpha)Q\omega(\alpha)\mathrm{d}\alpha \geq \left(\int_0^{\lambda}\omega(\alpha)\mathrm{d}\alpha\right)^T Q\left(\int_0^{\lambda}\omega(\alpha)\mathrm{d}\alpha\right).$$

Lemma 2 ([19]): Given a positive matrix R, scalars $\nu_1 < \nu_2$, the continuous function $\omega \in [\nu_1,\nu_2] \to \mathbb{R}^n$, the following inequality holds:

$$\int_{\nu_1}^{\nu_2} \omega(u)R\omega(u)\mathrm{d}u \geq \frac{1}{\nu_2-\nu_1}\Lambda^T R\Lambda + \frac{3}{\nu_2-\nu_1}\Psi^T R\Psi \tag{17}$$

where $\Psi = \int_{\nu_1}^{\nu_2}\omega(s)\mathrm{d}s - \frac{2}{\nu_2-\nu_1}\int_{\nu_1}^{\nu_2}\int_{\nu_1}^{s}\omega(r)\mathrm{d}r\mathrm{d}s$ and $\Lambda = \int_{\nu_1}^{\nu_2}\omega(u)\mathrm{d}u$.

III. Main Results

In this section, sufficient conditions will be derived by the utilization of Lyapunov functional approach, involving uncertain system parameters and actuator failures. The designed controller gain will be determined to guarantee the ISS of the system (14).

For system (14), similar to [14], consider the following Lyapunov function:

$$\mathbb{E}\{V_e(t)\} = \mathbb{E}\{V(t) + V_Q(t)\}, t \in [t_k, t_{k+1}) \tag{18}$$

where

$$V(t) = \tilde{V}(t) + V_G(t), V_Q(t) = \int_\Omega \sum_{i=1}^N e_i^T(x,t)Q_i e_i(x,t)\mathrm{d}x$$

$$\begin{aligned}\tilde{V}(t) = &\int_\Omega z^T(x,t)P_m z(x,t)\mathrm{d}x \\ &+ \int_\Omega\int_{t-\tilde{\eta}_m}^{t} \lambda z^T(x,\varpi)S_0 z(x,\varpi)\mathrm{d}\varpi\mathrm{d}x \\ &+ \int_\Omega\int_{t-\tau_M}^{t-\tilde{\eta}_m} \lambda z^T(x,\varpi)S_1 z(x,\varpi)\mathrm{d}\varpi\mathrm{d}x \\ &+ \int_\Omega\int_{t-\tilde{\eta}_m}^{t}\int_\theta^t \lambda\tilde{\eta}_m \dot{z}_\varpi^T(x,\varpi)R_0\dot{z}_\varpi(x,\varpi)\mathrm{d}\varpi\mathrm{d}\theta\mathrm{d}x \\ &+ \int_\Omega\int_{t-\tau_M}^{t-\tilde{\eta}_m}\int_\theta^t \lambda\epsilon\dot{z}_\varpi^T(x,\varpi)R_1\dot{z}_\varpi(x,\varpi)\mathrm{d}\varpi\mathrm{d}\theta\mathrm{d}x \\ &+ \int_\Omega z_x^T(x,t)Zz_x(x,t)\mathrm{d}x\end{aligned}$$

$$V_G(t) = \int_\Omega\sum_{i=1}^N\int_{s_k}^t \lambda\epsilon\dot{z}_\varpi^T(x,\varpi)C_i^T G_i C_i\dot{z}_\varpi(x,\varpi)\mathrm{d}\varpi\mathrm{d}x$$

$\lambda \triangleq e^{2\alpha(\varpi-t)}$, $\epsilon \triangleq \tau_M - \tilde{\eta}_m, \alpha > 0, P_m > 0, G_i > 0, Q_i > 0, S_j > 0, R_j > 0, i = 1,\ldots,N, m = 1,\ldots,M$, and $j = 1,2$.

To derive the sufficient stabilization criterion for the ISS of system (14), the following lemma is introduced.

Lemma 3 ([15]): Suppose that there exist constants $\alpha > 0$ and $\tilde{\gamma} > 0$, matrices $Q_i, U_i, G_i > 0, i = 1,\ldots,N$ and $V_e(t), t \in [t_k, t_{k+1})$ such that along (14) the following inequality:

$$\begin{aligned}\mathbb{E}\Bigg\{&\dot{V}_e(t) + 2\alpha V_e(t) - \int_\Omega \tilde{\gamma}^2 v^T(x,t)v(x,t)\mathrm{d}x \\ &- \frac{1}{\epsilon}\int_\Omega\sum_{i=1,i\neq\sigma_k}^N e_i^T(x,t)U_i e_i(x,t)\mathrm{d}x \\ &- \int_\Omega 2\alpha e_{\sigma_k}^T(x,t)Q_{\sigma_k}e_{\sigma_k}(x,t)\mathrm{d}x\Bigg\} \leq 0\end{aligned} \tag{19}$$

holds. Assume additionally that for $i = 1,\ldots,N$

$$\Omega_i = \begin{bmatrix} U_i - \frac{1-2\alpha\epsilon}{N-1}Q_i & * \\ Q_i & -G_i e^{-2\alpha\tau_M} + Q_i\end{bmatrix} < 0. \tag{20}$$

Then

$$\begin{aligned}\mathbb{E}\Bigg\{&V_e(x,t_{k+1}) + \int_\Omega 2\alpha\epsilon e_{\sigma_k}^T(x,t)Q_{\sigma_k}e_{\sigma_k}(x,t)\mathrm{d}x \\ &- V_e(t_{k+1}^-) + \int_\Omega\sum_{i=1,i\neq\sigma_k}^N e_i^T(x,t)U_i e_i(x,t)\mathrm{d}x\Bigg\} \leq 0\end{aligned} \tag{21}$$

holds. Moreover, one can get the following bounds for the solutions of (14) initialized by $z(t_0) \in [t_0 - \tau_m, t_0]$:

$$\mathbb{E}\{V(t)\} \leq e^{-2\alpha(t-t_0)}\mathbb{E}\{V_e(t_0)\} + \frac{\tilde{\gamma}^2}{2\alpha}J^2,\ t \geq t_0 \tag{22}$$

$$\mathbb{E}\{V_e(t_0)\} = V(t_0) + \int_\Omega\sum_{i=1}^N e_i^T(x,t_0)Q_i e_i(x,t_0)\mathrm{d}x \tag{23}$$

$$\int_\Omega\sum_{i=1}^N e_i^T(x,t)Q_i e_i(x,t)\mathrm{d}x \leq \frac{\tilde{\gamma}^2}{2\alpha}J^2 + \tilde{b}e^{-2\alpha(t-t_0)}\mathbb{E}\{V_e(t_0)\} \tag{24}$$

where $\tilde{b} = e^{2\alpha\epsilon}$, implying the ISS of system (14).

Proof: See appendix A.

Theorem 1: For the given scalars $\tau_M > \tilde{\eta}_m \geq 0, \alpha > 0, \delta > 0$, and $\gamma > 0$, the uncertain PDE system (14) is said to be ISS, if there exist matrices $Q_i > 0$, $P_m > 0$, $S_j > 0$, $R_j > 0$, $Z > 0$, $G_i > 0$, and $U_i > 0$ and K_{im} of appropriate dimensions, such that (20) combined with the following inequality is feasible for

$i=1,\ldots,N, m=1,\ldots,M$, and $j=1,2$:

$$\Xi=\begin{bmatrix}\Xi_{11} & * & * & * & * & * \\ \Xi_{21} & \Xi_{22} & * & * & * & * \\ \Xi_{31} & \Xi_{32} & \Xi_{33} & * & * & * \\ 0 & 0 & \Xi_{43} & \Xi_{44} & * & * \\ \Xi_{51} & 0 & 0 & 0 & \Xi_{55} & * \\ \Xi_{61} & 0 & \Xi_{63} & 0 & 0 & \Xi_{66}\end{bmatrix}<0 \tag{25}$$

where

$$\Xi_{11}=\begin{bmatrix}\Theta_{11} & * & * & * & * & * & * \\ \Theta_{21} & \Theta_{22} & * & * & * & * & * \\ \Theta_{31} & \Theta_{32} & \Theta_{33} & * & * & * & * \\ 0 & 0 & \Theta_{43} & \Theta_{44} & * & * & * \\ \Theta_{51} & \Theta_{52} & 0 & 0 & \Theta_{55} & * & * \\ 0 & \Theta_{62} & \Theta_{63} & 0 & 0 & \Theta_{66} & * \\ 0 & 0 & \Theta_{73} & \Theta_{74} & 0 & 0 & \Theta_{77}\end{bmatrix}$$

$$\Theta_{11}=S_0-4e^{-2\alpha\tilde{\eta}_m}R_0+2\alpha P_m+\sum_{n=1}^{M}\pi_{mn}P_n + \delta\left(ZA+A^TZ\right),\quad \Theta_{21}=-2e^{-2\alpha\tilde{\eta}_m}R_0$$

$$\Theta_{22}=e^{-2\alpha\tilde{\eta}_m}\left(S_1-S_0-4R_0\right)-4e^{-2\alpha\tau_m}R_1$$

$$\Theta_{31}=\sum_{i=1}^{N}\left(\delta ZBF_mK_{im}C_i\right)^T,\quad \Theta_{32}=-2e^{-2\alpha\tau_M}R_1$$

$$\Theta_{33}=-8e^{-2\alpha\tau_M}R_1,\quad \Theta_{66}=\Theta_{77}=-12e^{-2\alpha\tau_M}R_1$$

$$\Theta_{43}=-2e^{-2\alpha\tau_M}R_1,\quad \Theta_{44}=-e^{-2\alpha\tau_M}(S_1+4R_1)$$

$$\Theta_{51}=\Theta_{52}=6e^{-2\alpha\tilde{\eta}_m}R_0,\quad \Theta_{55}=-12e^{-2\alpha\tilde{\eta}_m}R_0$$

$$\Theta_{62}=\Theta_{63}=\Theta_{73}=\Theta_{74}=6e^{-2\alpha\tau_M}R_1$$

$$\gamma_i=\begin{bmatrix}(\delta ZBF_mK_{im}C_i)^T & 0 & 0 & 0 & 0 & 0 & 0\end{bmatrix}$$

$$\Xi_{21}=\begin{cases}\left[\gamma_2^T,\ldots,\gamma_N^T\right]^T, & \sigma_k=1\\ \left[\gamma_1^T,\ldots,\gamma_{\sigma_{k-1}}^T,\gamma_{\sigma_{k+1}}^T,\ldots,\gamma_N^T\right]^T, & \sigma_k\neq 1,N\\ \left[\gamma_1^T,\ldots,\gamma_{N-1}^T\right]^T, & \sigma_k=N\end{cases}$$

$$\varkappa_i=2\alpha C_i^TQ_iC_i-\frac{1}{\epsilon}C_i^TU_iC_i$$

$$\Xi_{22}=\begin{cases}\mathrm{diag}\{\varkappa_1,\ldots,\varkappa_N\}, & \sigma_k=1\\ \mathrm{diag}\{\varkappa_1,\ldots,\varkappa_{\sigma_{k-1}},\varkappa_{\sigma_{k+1}},\ldots,\varkappa_{\sigma_N}\}, & \sigma_k\neq 1,N\\ \mathrm{diag}\{\varkappa_1,\ldots\varkappa_{N-1}\}, & \sigma_k=N\end{cases}$$

$$\Xi_{31}=\begin{bmatrix}0 & 0 & 0 & 0 & 0 & 0 & 0\\ \Xi_{311} & 0 & \Xi_{312} & 0 & 0 & 0 & 0\end{bmatrix}$$

$$\Xi_{311}=P_m-\delta Z+ZA,\quad \Xi_{312}=\sum_{i=1}^{N}ZBF_mK_{im}C_i$$

$$\iota_i=\begin{bmatrix}0 & (ZBF_mK_{im}C_i)^T\end{bmatrix}^T$$

$$\Xi_{32}=\begin{cases}\left[\iota_2^T,\ldots,\iota_N^T\right]^T, & \sigma_k=1\\ \left[\iota_1^T,\ldots,\iota_{\sigma_{k-1}}^T,\iota_{\sigma_{k+1}}^T,\ldots,\iota_N^T\right]^T, & \sigma_k\neq 1,N\\ \left[\iota_1^T,\ldots,\iota_{N-1}^T\right]^T, & \sigma_k=N\end{cases}$$

$$\Xi_{33}=\mathrm{diag}\{2(\alpha-\delta)Z,\Xi_{331}\}$$

$$\Xi_{331}=\tilde{\eta}_m^2S_0-2Z+(\tau_m-\tilde{\eta}_m)^2S_1 + \sum_{i=1}^{N}(\tau_M-\tilde{\eta}_m)C_i^TG_iC_i$$

$$\Xi_{43}=\begin{bmatrix}0 & H^TZ\\ 0 & \gamma E\end{bmatrix},\quad \Xi_{44}=\mathrm{diag}\{-\gamma I,-\gamma I\}$$

$$\Xi_{51}=\begin{bmatrix}\delta H^TZ & 0 & 0 & 0 & 0 & 0 & 0\\ \gamma\delta E & 0 & 0 & 0 & 0 & 0 & 0\end{bmatrix},$$

$$\Xi_{55}=\mathrm{diag}\{-\gamma\delta I,-\gamma\delta I\}$$

$$\Xi_{61}=\begin{bmatrix}\delta L_mB^TZ & 0 & 0 & 0 & 0 & 0 & 0\end{bmatrix}$$

$$\Xi_{63}=\begin{bmatrix}0 & L_mB^TZ\end{bmatrix},\quad \Xi_{66}=-I.$$

Proof: See Appendix B for the detailed proofs.

Based on Theorem 1, a scheme to design on the security controller gains is provided in Theorem 2.

Theorem 2: For the given scalars $\tau_M>\tilde{\eta}_m\geq 0$, $\alpha>0$, $\delta>0$, and $\gamma>0$, the controller gains of uncertain PDE system (14) can be determined by $K_{im}=Y_{im}\Phi_i^{-1}$ and the weighted matrices $Q_i=(C_iC_i^T)^{-1}C_iX^{-1}\tilde{Q}_iX^{-1}C_i^T(C_iC_i^T)^{-1}$, if there exists scalars $\gamma>0$ and matrices $X>0$, $\tilde{P}_m>0$, $\tilde{S}_j>0$, $\tilde{R}_j>0$, $\tilde{G}_i>0$, $\tilde{Q}_i>0$, $\tilde{U}_i>0$, Y_{im}, and Φ_i, for $i=1,\ldots,N$, $m=1,\ldots,M$, $j=1,2$, such that

$$\tilde{\Xi}=\begin{bmatrix}\tilde{\Xi}_{11} & * & * & * & * & * \\ \tilde{\Xi}_{21} & \tilde{\Xi}_{22} & * & * & * & * \\ \tilde{\Xi}_{31} & \tilde{\Xi}_{32} & \tilde{\Xi}_{33} & * & * & * \\ 0 & 0 & \tilde{\Xi}_{43} & \Xi_{44} & * & * \\ \tilde{\Xi}_{51} & 0 & 0 & 0 & \Xi_{55} & * \\ \tilde{\Xi}_{61} & 0 & \tilde{\Xi}_{63} & 0 & 0 & \Xi_{66}\end{bmatrix}<0 \tag{26}$$

$$C_iX=\Phi_iC_i \tag{27}$$

where

$$\tilde{\Xi}_{11}=\begin{bmatrix}\tilde{\Theta}_{11} & * & * & * & * & * & * \\ \tilde{\Theta}_{21} & \tilde{\Theta}_{22} & * & * & * & * & * \\ \tilde{\Theta}_{31} & \tilde{\Theta}_{32} & \tilde{\Theta}_{33} & * & * & * & * \\ 0 & 0 & \tilde{\Theta}_{43} & \tilde{\Theta}_{44} & * & * & * \\ \tilde{\Theta}_{51} & \tilde{\Theta}_{51} & 0 & 0 & \tilde{\Theta}_{55} & * & * \\ 0 & \tilde{\Theta}_{62} & \tilde{\Theta}_{63} & 0 & 0 & \tilde{\Theta}_{66} & * \\ 0 & 0 & \tilde{\Theta}_{73} & \tilde{\Theta}_{74} & 0 & 0 & \tilde{\Theta}_{77}\end{bmatrix}$$

$$\tilde{\Theta}_{11}=\tilde{S}_0-4e^{-2\alpha\tilde{\eta}_m}\tilde{R}_0+2\alpha\tilde{P}_m+\sum_{n=1}^{M}\pi_{mn}\tilde{P}_n + \delta\left(AX+XA^T\right),\quad \tilde{\Theta}_{21}=-2e^{-2\alpha\tilde{\eta}_m}\tilde{R}_0$$

$$\tilde{\Theta}_{22} = e^{-2\alpha\tilde{\eta}_m}\left(\tilde{S}_1 - \tilde{S}_0 - 4\tilde{R}_0\right) - 4e^{-2\alpha\tau_m}\tilde{R}_1$$

$$\tilde{\Theta}_{31} = \sum_{i=1}^{N}\left(\delta BF_m Y_{im} C_i\right)^T, \quad \tilde{\Theta}_{32} = -2e^{-2\alpha\tau_M}\tilde{R}_1$$

$$\tilde{\Theta}_{33} = -8e^{-2\alpha\tau_M}\tilde{R}_1, \quad \tilde{\Theta}_{66} = \tilde{\Theta}_{77} = -12e^{-2\alpha\tau_M}\tilde{R}_1$$

$$\tilde{\Theta}_{43} = -2e^{-2\alpha\tau_M}\tilde{R}_1, \quad \tilde{\Theta}_{44} = -e^{-2\alpha\tau_M}(\tilde{S}_1 + 4\tilde{R}_1)$$

$$\tilde{\Theta}_{51} = \tilde{\Theta}_{52} = 6e^{-2\alpha\tilde{\eta}_m}\tilde{R}_0, \quad \tilde{\Theta}_{55} = -12e^{-2\alpha\tilde{\eta}_m}\tilde{R}_0$$

$$\tilde{\Theta}_{62} = \tilde{\Theta}_{63} = \tilde{\Theta}_{73} = \tilde{\Theta}_{74} = 6e^{-2\alpha\tau_M}\tilde{R}_1$$

$$\tilde{\gamma}_i = \begin{bmatrix}(\delta BF_m Y_{im} C_i)^T & 0 & 0 & 0 & 0 & 0 & 0\end{bmatrix}$$

$$\tilde{\Xi}_{21} = \begin{cases}\left[\tilde{\gamma}_2^T, \ldots, \tilde{\gamma}_N^T\right]^T, & \sigma_k = 1\\ \left[\tilde{\gamma}_1^T, \ldots, \tilde{\gamma}_{\sigma_{k-1}}^T, \tilde{\gamma}_{\sigma_{k+1}}^T, \ldots, \tilde{\gamma}_N^T\right]^T, & \sigma_k \neq 1, N\\ \left[\tilde{\gamma}_1^T, \ldots, \tilde{\gamma}_{N-1}^T\right]^T, & \sigma_k = N\end{cases}$$

$$\tilde{\varkappa}_i = 2\alpha\tilde{Q}_i - \frac{1}{\epsilon}\tilde{U}_i, \quad \tilde{\iota}_i = \begin{bmatrix}0 & (BF_m Y_{im} C_i)^T\end{bmatrix}^T$$

$$\tilde{\Xi}_{22} = \begin{cases}\text{diag}\{\tilde{\varkappa}_1, \ldots, \tilde{\varkappa}_N\}, & \sigma_k = 1\\ \text{diag}\{\tilde{\varkappa}_1, \ldots, \tilde{\varkappa}_{\sigma_{k-1}}, \tilde{\varkappa}_{\sigma_{k+1}}, \ldots, \tilde{\varkappa}_{\sigma_N}\}, & \sigma_k \neq 1, N\\ \text{diag}\{\tilde{\varkappa}_1, \ldots \tilde{\varkappa}_{N-1}\}, & \sigma_k = N\end{cases}$$

$$\tilde{\Xi}_{31} = \begin{bmatrix}0 & 0 & 0 & 0 & 0 & 0 & 0\\ \tilde{\Xi}_{311} & 0 & \tilde{\Xi}_{312} & 0 & 0 & 0 & 0\end{bmatrix},$$

$$\tilde{\Xi}_{311} = \tilde{P}_m - \delta X + AX, \quad \tilde{\Xi}_{312} = \sum_{i=1}^{N} BF_m Y_{im} C_i,$$

$$\tilde{\Xi}_{32} = \begin{cases}\left[\tilde{\iota}_2^T, \ldots, \tilde{\iota}_N^T\right]^T, & \sigma_k = 1\\ \left[\tilde{\iota}_1^T, \ldots, \tilde{\iota}_{\sigma_{k-1}}^T, \tilde{\iota}_{\sigma_{k+1}}^T, \ldots, \tilde{\iota}_N^T\right]^T, & \sigma_k \neq 1, N\\ \left[\tilde{\iota}_1^T, \ldots, \tilde{\iota}_{N-1}^T\right]^T, & \sigma_k = N\end{cases}$$

$$\tilde{\Xi}_{33} = \text{diag}\{2(\alpha - \delta)X, \tilde{\Xi}_{331}\},$$

$$\tilde{\Xi}_{331} = \tilde{\eta}_m^2\tilde{S}_0 - 2X + (\tau_m - \tilde{\eta}_m)^2\tilde{S}_1 + \sum_{i=1}^{N}(\tau_M - \tilde{\eta}_m)C_i^T\tilde{G}_i C_i, \ \tilde{\Xi}_{43} = \begin{bmatrix}0 & H^T\\ 0 & \gamma EX\end{bmatrix}$$

$$\tilde{\Xi}_{51} = \begin{bmatrix}\delta H^T & 0 & 0 & 0 & 0 & 0 & 0\\ \gamma\delta EX & 0 & 0 & 0 & 0 & 0 & 0\end{bmatrix}$$

$$\tilde{\Xi}_{61} = \begin{bmatrix}\delta L_m B^T & 0 & 0 & 0 & 0 & 0 & 0\end{bmatrix}$$

$$\tilde{\Xi}_{63} = \begin{bmatrix}0 & L_m B^T\end{bmatrix}, \quad \Xi_{66} = -I.$$

Proof: Define $X = Z^{-1}$, $\tilde{P}_m = XP_mX$, $\tilde{S}_j = XS_jX$, $\tilde{R}_j = XR_jX$, $\tilde{G}_i = X\Phi_i^T G_i\Phi_i X$, $\tilde{Q}_i = XC_i^T Q_i C_i X$, $\tilde{U}_i = XC_i^T U_i C_i X$, and $Y_{im} = K_{im}\Phi_i$. Premultiplying and postmultiplying (25) with diag$\{X, X, X, X, X, X, X, X, I, X, I, I, I\}$ and their transposes and combining (27), we have (26). Obviously, (25) is a sufficient condition to guarantee (26) holds. Then, the value of Y_{im} can be determined by solving (26). Furthermore, we can get controller gains $K_{im} = Y_{im}\Phi_i^{-1}$ and weighted matrices $Q_i = (C_iC_i^T)^{-1}C_iX^{-1}\tilde{Q}_iX^{-1}C_i^T(C_iC_i^T)^{-1}$.

Remark 4: In practical systems, such as industrial control, remote healthcare, and intelligent transportation, data transmission may encounter constraints. Therefore, the WTOD protocol for scheduling data transmission is utilized to prevent data collisions in this article. Note that, the system stability can be affected by WTOD protocol, system-related parameters, noise information, as well as actuator faults, these factors have been reflected in Theorems 1 and 2.

Remark 5: From Theorem 2, the feasibility of the linear matrix inequalities (LMIs) is related to the parameters τ_M, $\tilde{\eta}_m$, α, δ, and γ. In general, the complexity of the linear matrix inequality (LMI) computations is polynomial time bounded by $O(\mathcal{R}\mathcal{N}^3\log(\mathcal{C}/\vartheta))$, where $\mathcal{R}$ is the total row size of the LMIs, $\mathcal{N}$ is the number of scalar decision variables, $\mathcal{C}$ is the scaling factor, and ϑ is the relative accuracy set for the algorithm. Here, we assume that the system dimension is $\mathbf{n}$ and that the involved variable dimensions can be determined by Q_i, P_m, S_j, R_j, Z, G_i, U_i, and Y_{im}. Then, for Theorem 2, $\mathcal{R} = 18\mathbf{n}$ and $\mathcal{N} = 3\mathbf{n}^2 + 3\mathbf{n}$. Thus, the computational complexity of Theorem 3 can be expressed as $O(\mathbf{n}^7)$, which polynomially depends on the size of the PDE system. In addition, to reduce the conservatism of the proposed controller design method, it is effective to obtain the largest possible $\tilde{\eta}_m$ and the smallest possible τ_M based on the network transmission conditions in practical scenarios, while ensuring feasibility of the LMIs.

IV. Simulation Example

In this section, a practical example of boiler tube in the power plant is employed to validate the effectiveness of the designed control method. Temperature stability of the boiler tube is crucial for the safe operation of the power plant. Therefore, effective control of the tube wall temperature by the cooling medium at the top or bottom of the tube is essential to prevent overheating, carrying significant importance. Given the small diameter of the cylindrical slender boiler tube where heat transfer occurs predominantly radially, and considering the random factors in the environment, the temperature distribution of the tube can be abstracted into the following metal rod heat conduction model:

$$\frac{\partial\varphi(x,t)}{\partial t} = D\frac{\partial^2\varphi(x,t)}{\partial x^2} + (A + \Delta A)\varphi(x,t) + Bu^f(x,t)$$

where $\varphi(x,t)$ is the temperature distribution of the metal rod; $D = k/\rho C_i$ is the thermal diffusivity determined by density ρ, specific heat C_i, and thermal conductivity coefficient k; A denotes internal temperature effects; ΔA represents uncertain environmental factors.

The parameters of the coefficient matrix are chosen as $A = -0.72$, $B = 0.24$, $C = [0.85 \quad 0.73 \quad 0.94]^T$, and $D = I$. In the first actuator failure mode, $F_1 = 1$, $L_1 = 0.12$, and in the other mode, $F_2 = 1$, $L_2 = 0.15$. The switching time between $m = 2$ fault modes is determined by a Markov process, with the transition probability matrix $\Pi_1 = \begin{bmatrix}-3.4 & 3.4\\ 2.0 & -2.0\end{bmatrix}$.

In this article, we assume that the variable x takes values from 0 to 1. Discretizing variable x into 11 points,

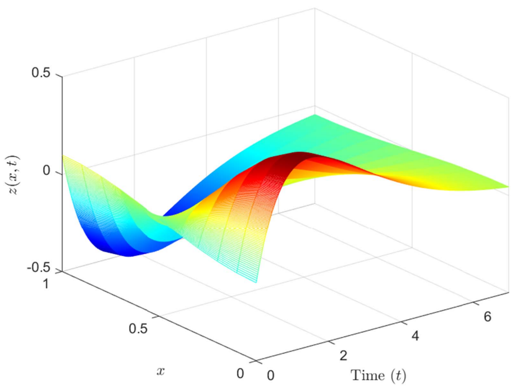

Fig. 2. State responses of the closed-loop system.

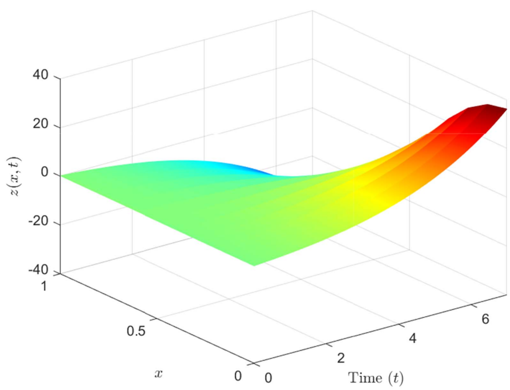

Fig. 3. State responses of the open-loop system.

that is $x \in \{0, 0.1, 0.2, 0.3, 0.4, 0.5, 0.6, 0.7, 0.8, 0.9, 1\}$. Setting $\tilde{\eta}_m = 0.02, \tau_M = 0.2, \alpha = 0, \delta = 0.98, \gamma = 0.81$, according to Theorem 3, using the LMI toolbox, we can derive the controller gains

$$K_{11} = -0.0033,\ K_{21} = -0.0038,\ K_{31} = -0.0063$$
$$K_{12} = -0.0039,\ K_{22} = -0.0045,\ K_{32} = -0.0068$$

and weighted matrices

$$Q_1 = 1.1958, \quad Q_2 = 1.6212, \quad Q_3 = 0.7788.$$

Fig. 2 shows the state response of the tube temperature with the designed control method in this article. The state responses of the open-loop system without control is depicted in Fig. 3. It proves the effectiveness of the controller designed in this article validated, which implies that the system is stable with respect to state $\varphi(x,t)$. Fig. 2 presents the state values of the system, from which it can be seen that the system state gradually approaches zero.

Fault occurrence and the switching of fault modes are displayed in Fig. 4. Fig. 5 illustrates the active nodes of transmission measurement data selected through the WTOD protocol. The scheduling of measurement data depend not only on the real-time transmission requirements of these sensor nodes but also on occurrences of actuator failures. Measurement data significantly affected by actuator failures will be prioritized for transmission via the WTOD protocol.

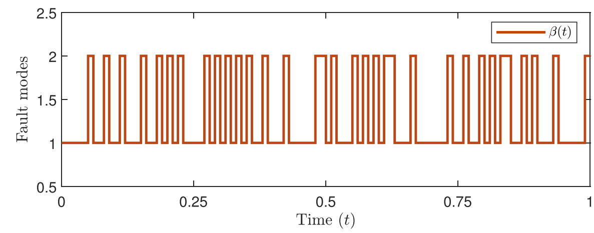

Fig. 4. Fault occurrence and fault mode $\beta(t)$ switching.

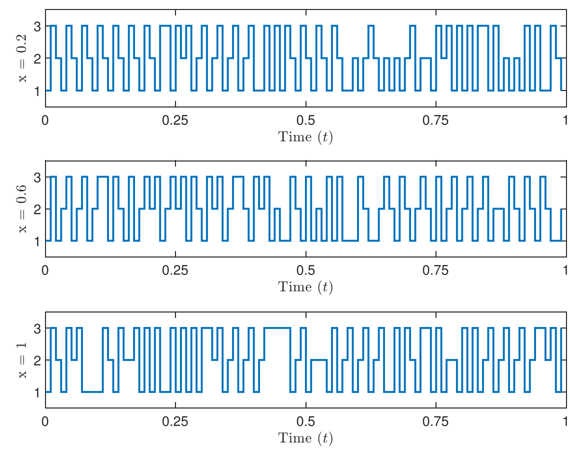

Fig. 5. Active node switching under the WTOD protocol.

TABLE I
DIFFERENT TIME DELAY BOUNDS $\tilde{\eta}_m$ AND τ_M

$\tilde{\eta}_m$	0.02	0.06	0.10	0.14	0.18	0.22
τ_M	0.20	0.45	0.70	0.95	1.10	1.2105

TABLE II
MEAN AND VARIANCE OF SYSTEM TEMPERATURE UNDER DIFFERENT TRANSITION PROBABILITY MATRIX

Transition Matrix	Temperature Mean	Temperature Variance
Π_1	-0.0012	0.0336
Π_2	-0.0009	0.0215
Π_3	-0.0011	0.0398

Table I provides the values of different time delay bounds $\tilde{\eta}_m$ and τ_M, used in the simulation experiments. While maintaining stable temperature control, the maximum tolerable delay is found to be 1.2105. This value represents the upper bound for τ_M that ensures the system can still effectively stabilize the temperature within the desired range.

In this simulation, we investigate the impact of stochastic elements on the system state by examining the mean and variance of the temperature under different transition probability matrices. The results, presented in Table II, are based on simulations conducted using various Markov transition matrices Π_1, Π_2, and

Π_3 with $\Pi_2 = \begin{bmatrix} -2.1 & 2.1 \\ 1.4 & -1.4 \end{bmatrix}$ and $\Pi_3 = \begin{bmatrix} -1.3 & 1.3 \\ 1.6 & -1.6 \end{bmatrix}$. The simulation results presented in Table II are based on multiple Monte Carlo runs, where the temperature mean and variance are computed over several trials. Table II validates the effective control of the system temperature under different transition matrices, demonstrating the control performance to maintain stable temperature despite the inherent randomness in the fault mode transitions. The above simulation results validate the effectiveness of the designed control strategy in tube temperature control.

V. Conclusion

This article investigates the stability control problem of uncertain PDE systems under imperfect network conditions. The WTOD protocol is selected to schedule the node transmissions in order to avoid collisions caused by multiple channels. A Markov process is used to simulate the switching of different fault modes in the actuators. The weight matrix of the scheduling protocol and the controller gains are derived by solving linear matrix inequalities. Future work can focus on the stability control problem of PDE systems under network attacks and multipacket transmission.

Appendix A Proof of Lemma 3

Note that, $\int_{t_k}^{t} e^{-2\alpha(t-\varpi)}\mathrm{d}\varpi \leq \epsilon$ and $\dot{e}_i(t) = 0, t \in [t_k, t_{k+1})$, from (19), one can get

$$\mathbb{E}\{V_e(t)\} \leq \mathbb{E}\Bigg\{ e^{-2\alpha(t-t_k)}V_e(t_k) + \int_\Omega \sum_{i=1, i\neq\sigma_k}^{N} e_i^T(x,t_k)U_i \times e_i(x,t_k)\mathrm{d}x + \int_\Omega 2\alpha\epsilon e_{\sigma_k}^T(x,t_k)Q_{\sigma_k}e_{\sigma_k}(x,t_k)\mathrm{d}x + \frac{\tilde{\gamma}^2 J^2}{2\alpha}\Bigg\}. \tag{28}$$

Thus, we can derive from (21) and (28) that

$$\mathbb{E}\left\{\tilde{V}(t) + V_G(t)\right\} \leq e^{-2\alpha(t-t_k)}\mathbb{E}\{V_e(t_k)\} + \frac{\tilde{\gamma}^2 J^2}{2\alpha}. \tag{29}$$

Denote $\mathbb{E}\{V_e(t_{k+1}) + 2\alpha\epsilon\int_\Omega e_{\sigma_k}^T(x,t_k)Q_{\sigma_k}e_{\sigma_k}(x,t_k)\mathrm{d}x - V_e(t_{k+1}^-) + \int_\Omega \sum_{i=1,i\neq\sigma_k}^N e_i^T(x,t_k)U_i e_i(x,t_k)\mathrm{d}x\}$ as Θ.

Since $V(t_{k+1}) = V(t_{k+1}^-)$ and $e(x,t_{k+1}^-) = e(x,t_k)$, Θ can be rewritten as

$$\begin{aligned}\Theta = &\int_\Omega \sum_{i=1}^{N}\left|\sqrt{Q_i}e_i(x,t_{k+1})\right|^2 - \sum_{i=1}^{N}\left|\sqrt{Q_i}e_i(x,t_k)\right|^2\mathrm{d}x \\ &+ 2\alpha\epsilon\int_\Omega \left|\sqrt{Q_{\sigma_k}}e_{\sigma_k}(x,t_k)\right|^2\mathrm{d}x + V_G(t_{k+1}) \\ &+ \int_\Omega \sum_{i=1,i\neq\sigma_k}^{N}\left|\sqrt{U_i}e_i(x,t_k)\right|^2\mathrm{d}x - V_G(t_{k+1}^-). \end{aligned}\tag{30}$$

It is clear that

$$\begin{aligned}&\mathbb{E}\left\{V_G(t_{k+1}) - V_G(t_{k+1}^-)\right\} \\ &= \int_\Omega -\sum_{i=1}^{N}\int_{s_k}^{s_{k+1}}\lambda_1\epsilon\left|\sqrt{G_i}C_i\dot{z}_\varpi(x,\varpi)\right|^2\mathrm{d}\varpi\mathrm{d}x\end{aligned} \tag{31}$$

where $\lambda_1 \triangleq e^{2\alpha(\varpi - t_{k+1})}$. Then, taking $\int_{s_k}^{s_{k+1}}\lambda_1\mathrm{d}\varpi \geq e^{-2\alpha\tau_M}$ into account, based on Lemma 1, we find

$$\begin{aligned}&\mathbb{E}\left\{V_G(t_{k+1}) - V_G(t_{k+1}^-)\right\} \\ &\leq \int_\Omega -\sum_{i=1}^{N}e^{-2\alpha\tau_M}\left|\sqrt{G_i}C_i[z(x,s_k) - z(x,s_{k+1})]\right|^2\mathrm{d}x.\end{aligned} \tag{32}$$

Substitute (32) into (30)

$$\begin{aligned}\Theta \leq &\int_\Omega \sum_{i=1}^{N}\left|\sqrt{Q_i}e_i(x,t_{k+1})\right|^2 - \sum_{i=1}^{N}\left|\sqrt{Q_i}e_i(x,t_k)\right|^2\mathrm{d}x \\ &+ 2\alpha\epsilon\int_\Omega\left|\sqrt{Q_{\sigma_k}}e_{\sigma_k}(x,t_k)\right|^2 + \sum_{i=1,i\neq\sigma_k}^{N}\left|\sqrt{U_i}e_i(x,t_k)\right|^2\mathrm{d}x \\ &- \sum_{i=1}^{N}e^{-2\alpha\tau_M}\left|\sqrt{G_i}C_i[z(x,s_k) - z(x,s_{k+1})]\right|^2\mathrm{d}x.\end{aligned} \tag{33}$$

It can be deduced from (11) and (33) that

$$\Theta \leq \int_\Omega \sum_{i=1,i\neq\sigma_k}^{N}\zeta_i^T\Omega_i\zeta_i\mathrm{d}x \leq 0 \tag{34}$$

where $\zeta_i = \mathrm{col}\{e_i(x,t_k), C_i(z(x,s_k) - z(x,s_{k+1}))\}$.

According to the functional expression (29), we can obtain

$$\mathbb{E}\{V_e(t)\} \leq e^{-2\alpha(t-t_0)}\mathbb{E}\{V_e(t_0)\} \tag{35}$$

$$\int_\Omega \lambda_{\min}(P_m)\mathrm{d}x \leq \mathbb{E}\{V_e(t)\} \tag{36}$$

then the inequality (22) holds.

Moreover, similar to [15], we can get that (35) yields (24) easily.

Appendix B Proof of Theorem 1

Define $\bar{e}_i = z(x,s_k) - z(x,s_{k+1})$, $\xi(t,x) \triangleq \mathrm{col}\{z(x,t)\ z(x,t-\tilde{\eta}_m)\ z(x,t-\tau(t))\ z(x,t-\tau_M)\ \frac{1}{\tilde{\eta}_m}\int_{t-\tilde{\eta}_m}^{t}z(x,\varpi)\mathrm{d}\varpi\ \frac{1}{\tau(t)-\tilde{\eta}_m}\int_{t-\tau(t)}^{t-\tilde{\eta}_m}z(x,\varpi)\mathrm{d}\varpi\ \frac{1}{\tau_M-\tau(t)}\int_{t-\tau_M}^{t-\tau(t)}z(x,\varpi)\mathrm{d}\varpi\ \varsigma(x,t)\ z_x(x,t)\ z_t(x,t)\ I\ I\ I\ I\ v(x,t)\}$, in which

$$\varsigma(x,t) = \begin{cases}\mathrm{col}\{\bar{e}_2,\ldots,\bar{e}_N\}, & \sigma_k = 1\\ \mathrm{col}\{\bar{e}_1,\ldots,\bar{e}_{\sigma_{k-1}},\bar{e}_{\sigma_{k+1}},\ldots,\bar{e}_N\}, & \sigma_k \neq 1, N\\ \mathrm{col}\{\bar{e}_1,\ldots,\bar{e}_{N-1}\}, & \sigma_k = N.\end{cases}$$

Based on Lemmas 1 and 2, using Schur's complement, the following inequality holds for $t \in [t_k, t_{k+1})$:

$$\mathbb{E}\Bigg\{\dot{V}_e(t) + 2\alpha V_e(t) - \int_\Omega \tilde{\gamma}^2 v^T(x,t)v(x,t)\mathrm{d}x - \frac{1}{\epsilon}\int_\Omega \sum_{i=1,i\neq\sigma_k}^{N}\bar{e}_i^T(x,t)C_i^T U_i C_i\bar{e}_i(x,t)\mathrm{d}x$$

$$
\left. - \int_{\Omega} 2\alpha \bar{e}_{\sigma_k}^T(x,t) Q_{\sigma_k} \bar{e}_{\sigma_k}(x,t) \mathrm{d}x \right\}
$$
$$
\leq \int_{\Omega} \xi^T(x,t) \Xi \xi(x,t) \mathrm{d}x. \tag{37}
$$

From (25) and Schur's complement, inequality (19) holds. Thus, according to Lemma 3, the proof of Theorem 1 is completed.

References

[1] P. Wei, H.-X. Li, and S. Xie, "Spatial-construction-based abnormality detection and localization for distributed parameter systems," *IEEE Trans. Ind. Informat.*, vol. 18, no. 7, pp. 4707–4714, Jul. 2022.

[2] X. Lu, D. Xu, and W. Liu, "Development of spatiotemporal recurrent neural network for modeling of spatiotemporal processes," *IEEE Trans. Ind. Inform.*, vol. 17, no. 1, pp. 189–198, Jan. 2021.

[3] J. Deutscher and N. Gehring, "Output feedback control of coupled linear parabolic ODE–PDE–ODE systems," *IEEE Trans. Autom. Control*, vol. 66, no. 10, pp. 4668–4683, Oct. 2021.

[4] I. Karafyllis, N. Bekiaris-Liberis, and M. Papageorgiou, "Feedback control of nonlinear hyperbolic PDE systems inspired by traffic flow models," *IEEE Trans. Autom. Control*, vol. 64, no. 9, pp. 3647–3662, Sep. 2019.

[5] M. J. Colbrook, "Extending the unified transform: Curvilinear polygons and variable coefficient PDEs," *IMA J. Numer. Anal.*, vol. 40, no. 2, pp. 976–1004, 2020.

[6] M. Ghousein and E. Witrant, "Adaptive observer design for uncertain hyperbolic PDEs coupled with uncertain LTV ODEs; application to refrigeration systems," *Automatica*, vol. 154, 2023, Art. no. 111096.

[7] S. Ghantasala and N. H. El-Farra, "Robust actuator fault isolation and management in constrained uncertain parabolic PDE systems," *Automatica*, vol. 45, no. 10, pp. 2368–2373, 2009.

[8] M. Ye, Q.-L. Han, L. Ding, and S. Xu, "Fully distributed Nash equilibrium seeking for high-order players with actuator limitations," *IEEE/CAA J. Automatica Sinica*, vol. 10, no. 6, pp. 1434–1444, Jun. 2023.

[9] G. Chen, R. Vazquez, Z. Liu, and H. Su, "Backstepping control of an underactuated hyperbolic–parabolic coupled PDE system," *IEEE Trans. Autom. Control*, vol. 69, no. 2, pp. 1218–1225, Feb. 2024.

[10] Z.-H. Pang, C.-G. Xia, W.-F. Zhai, G.-P. Liu, and Q.-L. Han, "Networked active fault-tolerant predictive control for systems with random communication constraints and actuator/sensor faults," *IEEE Trans. Circuits Syst. II: Exp. Briefs*, vol. 69, no. 4, pp. 2166–2170, Apr. 2022.

[11] Q.-Q. Li, Z.-P. Wang, T. Huang, H.-N. Wu, H.-X. Li, and J. Qiao, "Fault-tolerant stochastic sampled-data fuzzy control for nonlinear delayed parabolic PDE systems," *IEEE Trans. Fuzzy Syst.*, vol. 31, no. 8, pp. 2679–2693, Aug. 2023.

[12] Y.-X. Li, X. Li, B. Xu, and S. Tong, "Adaptive actuator failure compensation control of uncertain nonlinear PDE-ODE cascaded systems," *IEEE Trans. Syst., Man, Cybern. Syst.*, vol. 53, no. 9, pp. 5751–5759, Sep. 2023.

[13] X.-X. Han, D. Efimov, A. Polyakov, and K.-N. Wu, "Finite-time ISS for reaction-diffusion systems via hybrid boundary feedback control," *Automatica*, vol. 160, 2024, Art. no. 111443.

[14] H. Yang, C. Peng, and Z. Cao, "Attack-model-independent stabilization of networked control systems under a jump-like TOD scheduling protocol," *Automatica*, vol. 152, 2023, Art. no. 110982.

[15] K. Liu, E. Fridman, and K. H. Johansson, "Networked control with stochastic scheduling," *IEEE Trans. Autom. Control*, vol. 60, no. 11, pp. 3071–3076, Nov. 2015.

[16] H. Liu, Z. Wang, W. Fei, and H. Dong, "On state estimation for discrete time-delayed memristive neural networks under the WTOD protocol: A resilient set-membership approach," *IEEE Trans. Syst., Man, Cybern. Syst.*, vol. 52, no. 4, pp. 2145–2155, Apr. 2022.

[17] J. Wang and Y. Song, "Resilient RMPC for cyber-physical systems with polytopic uncertainties and state saturation under TOD scheduling: An ADT approach," *IEEE Trans. Ind. Inform.*, vol. 16, no. 7, pp. 4900–4908, Jul. 2020.

[18] S. Xiao, X. Ge, Q.-L. Han, and Y. Zhang, "Resource-efficient platooning control of connected automated vehicles over VANETs," *IEEE Trans. Intell. Veh.*, vol. 7, no. 3, pp. 579–589, Sep. 2022.

[19] X. Song, M. Wang, C. K. Ahn, and S. Song, "Finite-time fuzzy bounded control for semilinear PDE systems with quantized measurements and Markov jump actuator failures," *IEEE Trans. Cybern.*, vol. 52, no. 7, pp. 5732–5743, Jul. 2022.

[20] T. Li, Y. Ma, and T. Endoh, "From algorithm to module: Adaptive and energy-efficient quantization method for edge artificial intelligence in IoT society," *IEEE Trans. Ind. Inform.*, vol. 19, no. 8, pp. 8953–8964, Aug. 2023.

[21] J.-W. Wang and H.-N. Wu, "Design of suboptimal local piecewise fuzzy controller with multiple constraints for quasi-linear spatiotemporal dynamic systems," *IEEE Trans. Cybern.*, vol. 51, no. 5, pp. 2433–2445, May 2021.

[22] J. Qiu, S. X. Ding, H. Gao, and S. Yin, "Fuzzy-model-based reliable static output feedback H_∞ control of nonlinear hyperbolic PDE systems," *IEEE Trans. Fuzzy Syst.*, vol. 24, no. 2, pp. 388–400, Apr. 2016.

[23] J. Liu, E. Gong, L. Zha, E. Tian, and X. Xie, "Observer-based security fuzzy control for nonlinear networked systems under weighted try-once-discard protocol," *IEEE Trans. Fuzzy Syst.*, vol. 31, no. 11, pp. 3853–3865, Nov. 2023.

[24] K. Gu, J. Chen, and V. L. Kharitonov, *Stability of Time-Delay Systems*. Berlin, Germany: Springer, 2003.

Jinliang Liu (Senior Member, IEEE) received the Ph.D. degree in control science and engineering from the School of Information Science and Technology, Donghua University, Shanghai, China, in 2011.

From 2011 to 2023, he was an Associate Professor and then a Professor with the Nanjing University of Finance and Economics, Nanjing, China. In June 2023, he joined the Nanjing University of Information Science and Technology, Nanjing, where he is currently a Professor with the School of Computer Science. His research interests include networked control systems, complex dynamical networks, and time delay systems.

Lijuan Zha received the Ph.D. degree in control science and engineering from Donghua University, Shanghai, China, in 2018.

From 2017 to 2024, she was an Associate Professor with the College of Information Engineering, Nanjing University of Finance and Economics, Nanjing, China. From 2018 to 2023, she was a Postdoctoral Research Associate with the School of Mathematics, Southeast University, Nanjing. She is currently a Professor with the College of Science, Nanjing Forestry University, Nanjing. Her current research interests include networked control systems, neural networks, and complex dynamical systems.

Wen Jiang, photograph and biography not available at the time of publication.

Engang Tian (Senior Member, IEEE) received the B.S. degree in mathematics from Shandong Normal University, Jinan, China, in 2002, the M.Sc. degree in operations research and cybernetics from Nanjing Normal University, Nanjing, China, in 2005, and the Ph.D. degree in control theory and control engineering from Donghua University, Shanghai, China, in 2008.

He is currently a Professor with the School of Optical-Electrical and Computer Engineering, University of Shanghai for Science and Technology, Shanghai. His research interests include networked control systems, cyber attack, as well as nonlinear stochastic control and filtering.